

# Supporting Information

Nieves-Cintrón *et al.* 10.1073/pnas.0808759105

## SI Materials and Methods

**Isolation of Arterial Myocytes.** Animals were handled in strict compliance with the guidelines of the University of Washington Institutional Animal Care and Use Committee. For this study, we used Sprague–Dawley (SD), spontaneous hypertensive rats (SHR) ( $\approx 250$  g), and WT and PKC $\alpha$  knockout (PKC $\alpha^{-/-}$ ) mice ( $\approx 25$  g). A lethal dose of sodium pentobarbital (250 mg/kg), was injected intraperitoneally for euthanasia. Myocytes were dissociated from cerebral (middle, posterior, and basilar) and mesenteric (second and third order) arteries by using standard enzymatic techniques (1). After dissociation, cells were maintained in nominally Ca $^{2+}$ -free Ringer's solution until used. Thapsigargin (1  $\mu$ M) was included in all solutions to eliminate Ca $^{2+}$  release from intracellular stores during experimentation.

**Cell Culture.** Primary cultures of human aortic smooth muscle cells were obtained from Lonza. These cells were cultured in smooth muscle cell basal medium with the following growth supplements: hEGF, insulin, hFGF-B, and FBS. Cell cultures were maintained at 37°C in 5% CO $_2$ . Cells between passages 6 and 12 were used for experiments.

**Angiotensin II Infusion and Blood Pressure Monitoring.** Angiotensin II was administered by means of Osmotic mini pumps (Alzet, Durect Corporation, Cupertino, CA). Rats were implanted with the Alzet 2002 model; the angiotensin II dose was 300 ng/kg/min (2). For WT and PKC $\alpha^{-/-}$  mice, we use the micro osmotic pump model 1007D with an angiotensin II dose of 800 ng/kg/min (3). For control purposes, osmotic minipumps eluting normal saline were used. Telemetry (Data Science International) was used to monitor blood pressure in conscious, freely moving mice before and after osmotic mini pump implantation as described previously (6). The dose of angiotensin II infusion used in our animal studies (i.e., 300–800 ng/kg/min) was selected because it induces reproducible hypertension (3–6). Other investigators have used a similar dose to induce hypertension (4, 5). Assuming a steady-state level of angiotensin II of  $\approx 24$  and 75 ng for a typical mouse (weight  $\approx 25$  g) and rat (weight  $\approx 250$  g) respectively, in 1 g of skeletal muscle ( $\approx 400$  ml of interstitial volume) (8), angiotensin II could, in principle, reach a concentration ranging between 60 and 190 nM. These values are within the range of interstitial angiotensin II concentration we used *in vitro* and reported by others *in vivo* during hypertension (11).

**Patch-Clamp Electrophysiology.** All Ca $^{2+}$  sparklet and L-type Ca $^{2+}$  currents ( $I_{Ca}$ ) recordings were performed in patch-clamp cells (whole-cell configuration) to control membrane voltage by using an Axopatch 200B amplifier. During experiments, cells were continuously superfused with a solution containing: 120 mM NMDG, 5 mM CsCl, 1 mM MgCl $_2$ , 10 mM glucose, 10 mM Hepes, and 20 mM CaCl $_2$  adjusted to pH 7.4. Pipettes were filled with a solution composed of 87 mM Cs-aspartate, 20 mM CsCl, 1 mM MgCl $_2$ , 5 mM MgATP, 10 mM Hepes, 10 mM EGTA, and adjusted to pH 7.2 with CsOH. For Ca $^{2+}$  sparklets experiments, 0.2 mM fluo-5F was added to the pipette solution. A voltage error of 10 mV attributable to liquid junction potential of these solutions was corrected for. Whole-cell L-type Ca $^{2+}$  currents were recorded during a step depolarization (200 ms) from the holding potential of  $-70$  mV to  $+30$  mV. Currents were sampled at 20 kHz and low-pass filtered at 2 kHz.

**Ca $^{2+}$  Sparklet Recordings.** Ca $^{2+}$  sparklets were recorded as previously described (9, 10). Briefly, we used a through-the-lens total internal reflection fluorescence (TIRF) microscope built around an inverted Olympus IX-70 microscope equipped with an Olympus PlanApo ( $\times 60$ , N.A. = 1.45) oil-immersion lens and an Andor iXON CCD camera. Cells were loaded with the calcium indicator fluo-5F with excitation achieved by the 488-nm line of an argon laser. Images were acquired at 100 Hz. As before (9, 10), we quantified Ca $^{2+}$  sparklet activity by calculating the  $nP_s$  of each Ca $^{2+}$  sparklet site, where  $n$  is the number of quantal levels, and  $P_s$  is the probability that a quantal Ca $^{2+}$  sparklet event is active. Using this analysis, we have grouped Ca $^{2+}$  sparklet sites into three categories: silent ( $nP_s$  of 0), low ( $nP_s$  between 0 and 0.2), and high ( $nP_s > 0.2$ ). A detailed description of this analysis can be found in Navedo *et al.* 2005 (9). We used signal mass analysis to quantify Ca $^{2+}$  influx associated with Ca $^{2+}$  sparklets (11, 12).

Fluo-5F fluorescence signals were converted to Ca $^{2+}$  concentration units by using the “ $F_{\max}$ ” equation (13),

$$[\text{Ca}^{2+}] = K_d \frac{F/F_{\max} - 1/R_f}{1 - F/F_{\max}}$$

as described in detail previously (10, 14). Briefly,  $F$  is fluorescence,  $F_{\max}$  is the fluorescence intensity of fluo-4/5F in the presence of saturating free Ca $^{2+}$ ,  $K_d$  is the dissociation constant of the indicator (fluo-5F = 1,280 nM; fluo-4 = 800 nM), and  $R_f$  is the indicator's  $F_{\max}/F_{\min}$  ratio (fluo-5F = 286; fluo-4 = 150).  $F_{\min}$  is the fluorescence intensity of the indicator in a solution where the Ca $^{2+}$  concentration is 0.  $K_d$  and  $R_f$  values were determined *in vitro* by using standard methods and are similar to those reported by others (15).  $F_{\max}$  was determined at the end of each experiment by exposing cells or arteries to the Ca $^{2+}$  ionophore ionomycin (10  $\mu$ M) and 20 mM external Ca $^{2+}$ .

**Arterial [Ca $^{2+}$ ]<sub>i</sub> Imaging and Pressurized Artery Diameter Measurements.** For arterial wall Ca $^{2+}$  imaging and pressurized artery diameter measurements, small mesenteric (types II and III) artery segments from WT and PKC $\alpha^{-/-}$  mice were dissected, cannulated, and mounted in a close-working-distance arteriograph. The arteriograph was placed on the stage of an inverted microscope; the artery was perfused extraluminally (3–6 ml/min) at 37°C with bicarbonate-based physiological saline solution composed of: 119 mM NaCl, 4.7 mM KCl, 24 mM NaHCO $_3$ , 1.2 mM KH $_2$ PO $_4$ , 1.6 mM CaCl $_2$ , 1.2 mM MgSO $_4$ , and 11 mM glucose with the pH set to 7.4 by bubbling with a gas mixture of O $_2$  (95%) and CO $_2$  (5%). Arterial wall [Ca $^{2+}$ ]<sub>i</sub> was imaged by using a Radiance 2100 confocal system coupled to a Nikon TE300 inverted microscope equipped with a Nikon  $\times 20$  (N.A. = 0.75) lens. Arteries were loaded with the Ca $^{2+}$  indicator fluo-4 as described (16). Intravascular pressure was maintained at 80 mmHg for these experiments. Fluo-4 fluorescence signals were converted to Ca $^{2+}$  concentration units by using the  $F_{\max}$  equation described above.

Internal diameters of pressurized arteries were measured from live video images with the length-calibrated edge-detection function of an IonOptix imaging software at a sampling rate of 1 Hz. Myogenic tone was assessed by subjecting the vessels to a series of pressure steps between 40 and 100 mmHg. Pressure steps were achieved by elevating or lowering an attached water reservoir and monitored by using a pressure transducer. Spontaneous myogenic tone was allowed to develop at each step. At

the end of each experiment, arteries were perfused with nominally  $\text{Ca}^{2+}$ -free bicarbonate-base solution containing 10  $\mu\text{M}$  diltiazem and the pressure steps repeated to obtain the artery passive diameter. Myogenic tone was calculated as the percent difference in active diameter versus passive diameter at each pressure. Angiotensin II-induced constriction was assessed by perfusing arteries pressurized to 80 mmHg with bicarbonate-base solution containing 100 nM angiotensin II. Angiotensin II-induced constriction was defined as the percent decrease in internal diameter after the application of the contractile stimuli versus passive diameter. For all of the experiments, arterial viability was tested by raising external  $[\text{K}^+]$  to 60 mM; arteries that failed to contract robustly in response to high  $[\text{K}^+]$  were discarded.

**PKC $\alpha$  Immunofluorescence Imaging.** Immunofluorescence labeling of dispersed myocytes was performed by using a monoclonal antibody that recognizes the  $\alpha$  isoform of PKC (Abcam) as described previously (1, 16). The secondary antibody was an Alexa Fluor 488-conjugated rabbit anti-mouse (5 mg/ml) from Molecular Probes. Cells were imaged by using our confocal system. Surface and cytosolic PKC $\alpha$ -associated immunofluorescence was quantified by measuring the intensity of pixels above a set threshold defined as the mean fluorescence intensity outside the cells (i.e., background) plus three times its standard deviation. For each cell, pixel intensities of the entire surface membrane ( $\approx 1 \mu\text{m}$  in width) and a spatially equivalent section of cytosol were obtained and averaged. From these measurements, we determined the ratio of surface to cytosolic PKC $\alpha$  and used this as an indicator of PKC $\alpha$  translocation and activity (17, 18).

**RT-PCR.** Human aortic smooth muscle cells were cultured under the following conditions: media, saline, AngII, AngII + Dilt, and AngII + VIVIT. We used the peptide VIVIT because it specifically inhibits NFAT signaling without affecting other signaling pathways activated by this phosphatase. Total RNA was isolated from cultured cells by using the RNeasy Mini kit (Quiagen) per the manufacturer's instructions. Total RNA was reverse transcribed by using the High-Capacity cDNA Reverse Transcription kit (Applied Biosystems) following manufacturer's instructions. Real-time PCR (RT-PCR) was performed using SYBR green (QuantiTect SYBR green PCR; Quiagen) as the fluorescence probe on an ABI 7700 sequence detector (PE;

Applied Biosystems). Cycling conditions were 95°C for 15 min, followed by 40 cycles of 94°C for 15 s; 55°C for 30 s, 72°C for 30 s. A set of commercial primers (SuperArray) were used to detect Kv2.1 transcript (accession no. NM\_004975.2; NT 867–885; amplicon = 122 bp).  $\beta$ -Actin expression (NM\_001101.3; NT 1202–1222; amplicon = 191) was used as an internal control. We also verified L-type  $\alpha$ -1C subunit expression (accession no. NM\_012517) with a commercial primer (SuperArray) that amplifies a sequence between NT 6548 and 6567 (amplicon = 164 bp). Specific primers (sense NT 2206–2223 and antisense NT 2885–2402; amplicon = 196) were designed to detect rat  $\beta$ -actin (accession no. V01217) transcript. Product quantization was performed by using the relative quantification method (19). To examine primer efficiencies, standard curves were generated for each primer pair by regression analysis of PCR amplifications of serial dilutions of the RT product. The relative abundance of the transcript was normalized to  $\beta$ -actin transcript expression.

**Measurement of Calcineurin and NFAT Activity.** Calcineurin activity in arterial smooth muscle from control and angiotensin II-treated WT and PKC $\alpha^{-/-}$  mice was assessed by using a colorimetric Calcineurin Cellular Activity Assay kit (Calbiochem, EMD Biosciences) following the manufacturer's instructions. NFATc3 translocation in response to PDBu was assessed in primary cultured human aortic smooth muscle cells (Lozan) transfected with NFATc3 fused to EGFP (NFATc3-EGFP) using an Amaxa nucleofector system. Cells were used 3 days after transfection and were serum deprived 24 h before experiments were conducted. To assess NFAT transcriptional activity in response to PKC activation, human aortic smooth muscle cells were transfected (as described above) with a construct in which EGFP expression is under the control of NFAT. EGFP fluorescence and  $[\text{Ca}^{2+}]_i$  were imaged by using a Radiance 2100 confocal system coupled to a Nikon TE300 inverted microscope equipped with a Nikon  $\times 20$  (N.A. = 0.75) lens. For  $[\text{Ca}^{2+}]_i$  recordings, human aortic smooth muscle cells were loaded with the  $\text{Ca}^{2+}$  indicator X-rhod 1 as described elsewhere (16).

**Chemicals and Statistics.** All chemicals were from Sigma–Aldrich unless stated otherwise. Normally distributed data are presented as mean  $\pm$  SEM. Two-sample comparisons were made by using a Student's *t* test. Nonparametric statistical analyses (Mann–Whitney test) were used for nonnormally distributed data. *P* values  $< 0.05$  were considered significant. Asterisks used in the figures indicate a significant difference between groups.

- Amberg GC, Santana LF (2003) Downregulation of the BK channel  $\beta 1$  subunit in genetic hypertension. *Circ Res* 93:965–971.
- Amberg GC, Santana LF (2006) Kv2 channels oppose myogenic constriction of rat cerebral arteries. *Am J Physiol* 291:C348–C356.
- Amberg GC, Rossow CF, Navedo MF, Santana LF (2004) NFATc3 regulates Kv2.1 expression in arterial smooth muscle. *J Biol Chem* 279:47326–47334.
- Ceravolo GS, et al. (2007) Angiotensin II chronic infusion induces B1 receptor expression in aorta of rats. *Hypertension* 50:756–761.
- Ryan MJ, Didion SP, Mathur S, Faraci FM, Sigmund CD (2004) Angiotensin II-induced vascular dysfunction is mediated by the AT1A receptor in mice. *Hypertension* 43:1074–1079.
- Nieves-Cintrón M, Amberg GC, Nichols CB, Molkenin JD, Santana LF (2007) Activation of NFATc3 down-regulates the  $\beta 1$  subunit of large conductance, calcium-activated  $\text{K}^+$  channels in arterial smooth muscle and contributes to hypertension. *J Biol Chem* 282:3231–3240.
- Khairallah PA, Page IH, Bumpus FM, Turker RK (1966) Angiotensin tachyphylaxis and its reversal. *Circ Res* 19:247–254.
- Sheff MF, Zacks SI (1982) Interstitial space of mouse skeletal muscle. *J Physiol* 328:507–519.
- Navedo MF, Amberg G, Votaw SV, Santana LF (2005) Constitutively active L-type  $\text{Ca}^{2+}$  channels. *Proc Natl Acad Sci USA* 102:11112–11117.
- Navedo MF, Amberg GC, Nieves M, Molkenin JD, Santana LF (2006) Mechanisms underlying heterogeneous  $\text{Ca}^{2+}$  sparklet activity in arterial smooth muscle. *J Gen Physiol* 127:611–622.
- Zou H, Lifshitz LM, Tuft RA, Fogarty KE, Singer JJ (2002) Visualization of  $\text{Ca}^{2+}$  entry through single stretch-activated cation channels. *Proc Natl Acad Sci USA* 99:6404–6409.
- Zou H, Lifshitz LM, Tuft RA, Fogarty KE, Singer JJ (2004) Using total fluorescence increase (signal mass) to determine the  $\text{Ca}^{2+}$  current underlying localized  $\text{Ca}^{2+}$  events. *J Gen Physiol* 124:259–272.
- Maravall M, Mainen ZF, Sabatini BL, Svoboda K (2000) Estimating intracellular calcium concentrations and buffering without wavelength ratioing. *Biophys J* 78:2655–2667.
- Dilly KW, et al. (2006) Mechanisms underlying variations in excitation-contraction coupling across the mouse left ventricular free wall. *J Physiol* 572:227–241.
- Woodruff ML, et al. (2002) Measurement of cytoplasmic calcium concentration in the rods of wild-type and transducin knock-out mice. *J Physiol* 542:843–854.
- Amberg GC, Navedo MF, Nieves-Cintrón M, Molkenin JD, Santana LF (2007) Calcium sparklets regulate local and global calcium in murine arterial smooth muscle. *J Physiol* 579:187–201.
- Khalil RA, Lajoie C, Morgan KG (1994) In situ determination of  $[\text{Ca}^{2+}]_i$  threshold for translocation of the alpha-protein kinase C isoform. *Am J Physiol* 266:C1544–C1551.
- Khalil RA, Morgan KG (1991) Imaging of protein kinase C distribution and translocation in living vascular smooth muscle cells. *Circ Res* 69:1626–1631.
- Pfaffl MW (2001) A new mathematical model for relative quantification in real-time RT-PCR. *Nucleic Acids Res* 29:e45.

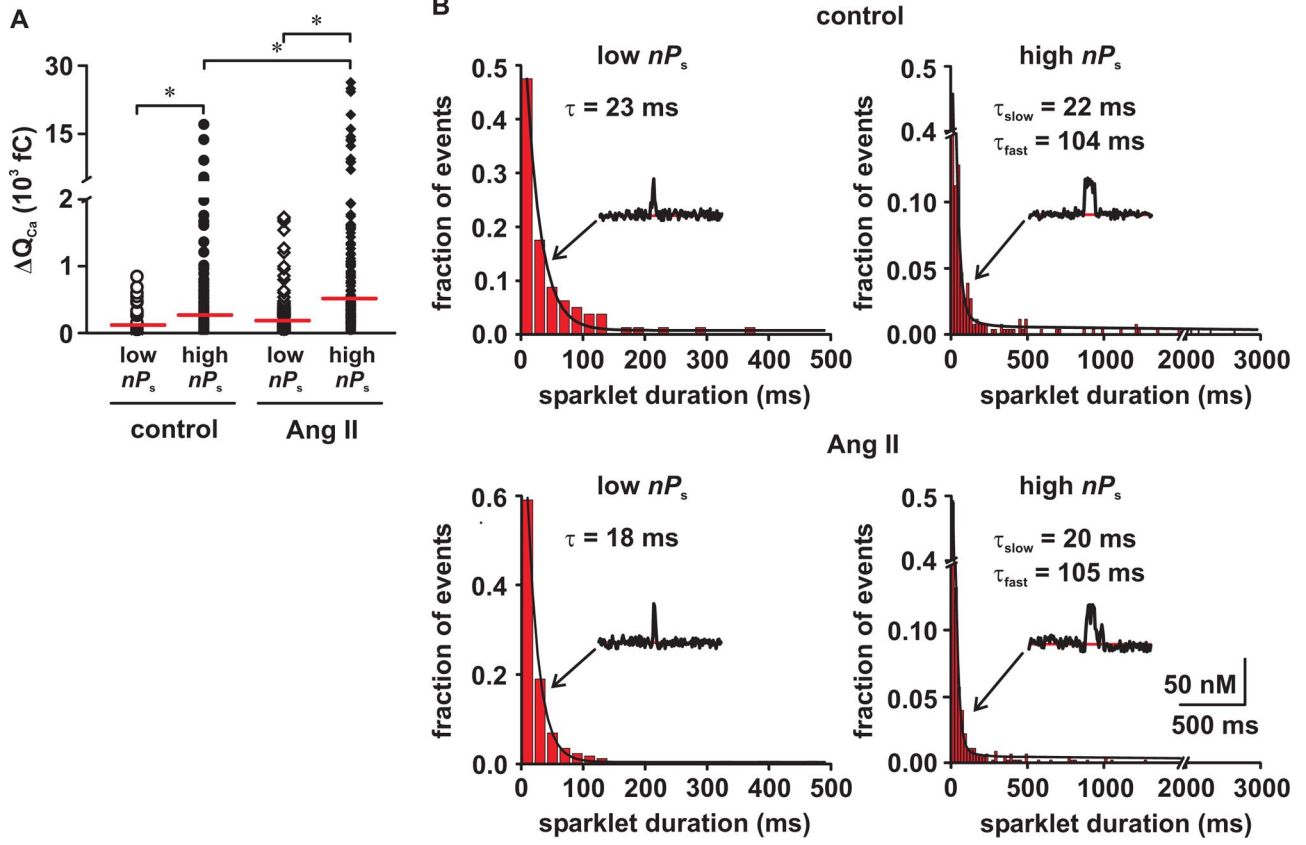


**Fig. 51.** Acute AngII application increases  $Ca^{2+}$  sparklet signal mass and activity. **(A)** Scatter plot of the signal mass of low and high  $nP_s$   $Ca^{2+}$  sparklets sites in arterial myocytes during control conditions and after AngII stimulation. **(B)** Histograms of the duration of low and high  $nP_s$   $Ca^{2+}$  sparklets sites in arterial myocytes during control (*Upper*) conditions and after AngII application (*Lower*). \*,  $P < 0.05$ .

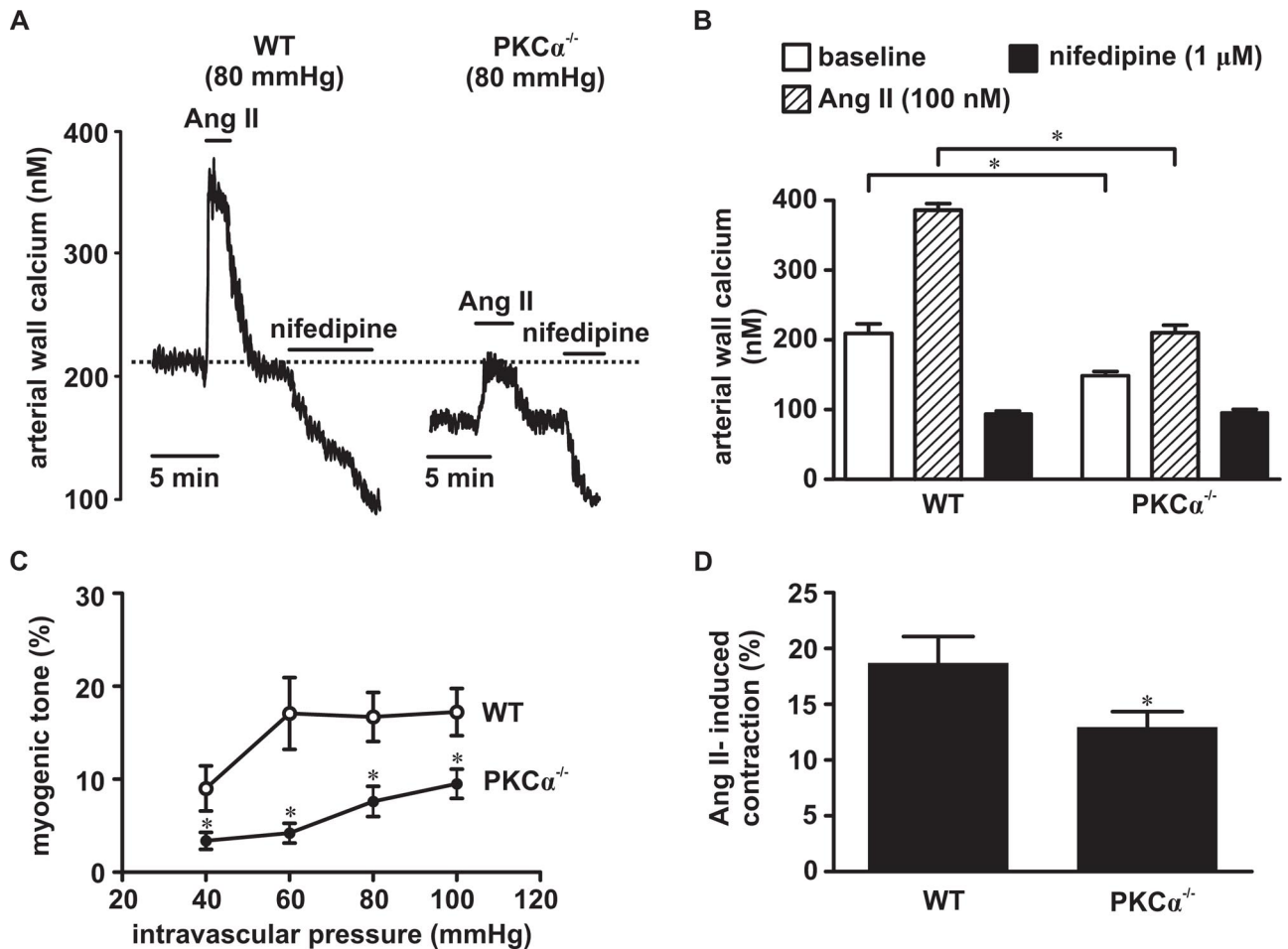


**Fig. S2.** Lower arterial wall  $[Ca^{2+}]_i$  and myogenic tone in pressurized PKC $\alpha^{-/-}$  than in WT arteries. (A) Time course of  $[Ca^{2+}]_i$  in pressurized (80 mmHg) WT and PKC $\alpha^{-/-}$  arteries during control conditions and after the application of 100 nM AngII or 1  $\mu$ M nifedipine. (B) Bar plot of the mean  $\pm$  SEM of the  $[Ca^{2+}]_i$  in WT ( $n = 5$ ) and PKC $\alpha^{-/-}$  ( $n = 5$ ) arteries under control conditions and after the application of 100 nM AngII or 1  $\mu$ M nifedipine. (C) Plot of myogenic tone as a function of intravascular pressure in WT ( $n = 6$ ) and PKC $\alpha^{-/-}$  ( $n = 6$ ) arteries. (D) Bar plot of the mean  $\pm$  SEM of AngII-induced contraction in pressurized (80 mmHg) WT and PKC $\alpha^{-/-}$  arteries. \*,  $P < 0.05$ .



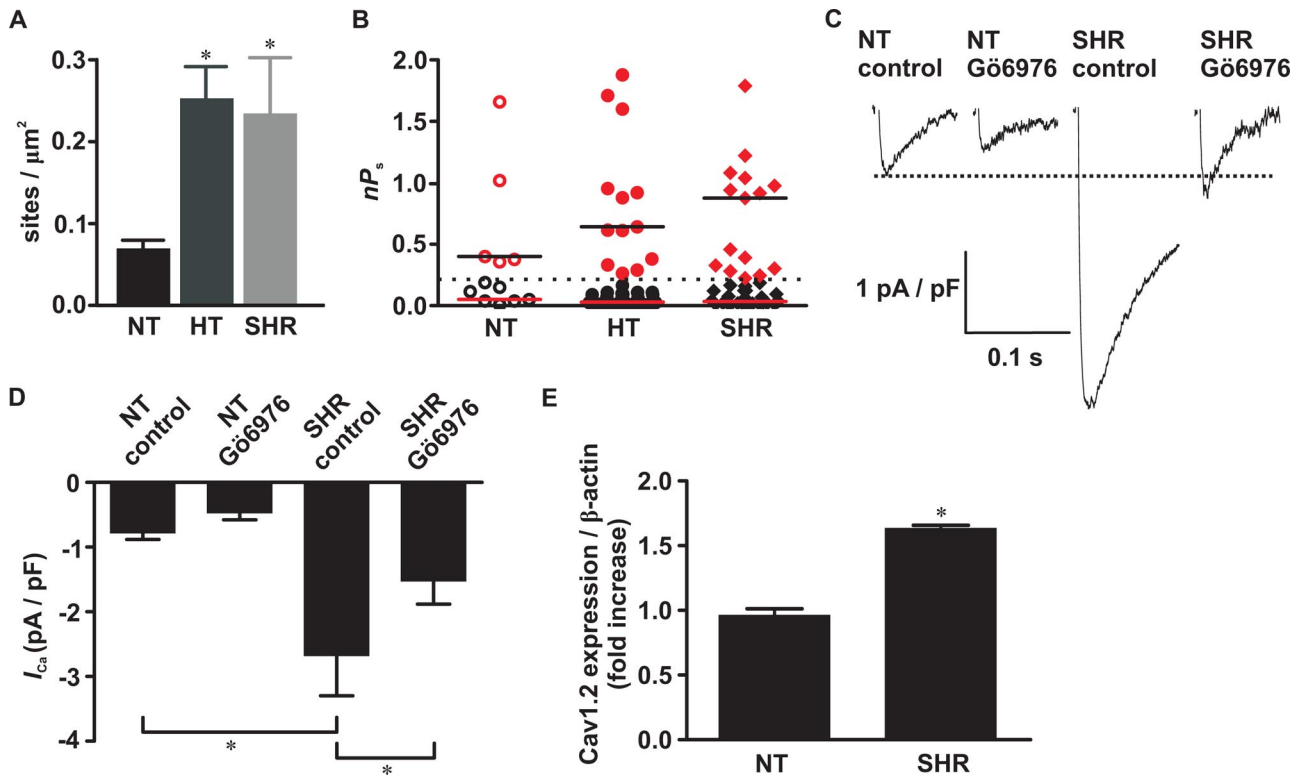


**Fig. 53.** Ca<sup>2+</sup> sparklet, I<sub>Ca</sub> and Cav1.2 expression is increased during genetic and AngII-induced hypertension. (A) Bar plot of Ca<sup>2+</sup> sparklet density in arterial smooth muscle cells NT, HT (AngII-induced hypertension), and SHR (n = 5). (B) Scatter plot of nP<sub>s</sub> values for individual Ca<sup>2+</sup> sparklet sites in NT, HT, and SHR arterial myocytes. (C) Representative L-type Ca<sup>2+</sup> channel whole-cell currents from NT and SHR arterial myocytes before and after exposure to Gö6976. (D) Bar plot of the mean ± SEM of I<sub>Ca</sub> density (at +30 mV and 20 mM Ca<sup>2+</sup>) in NT (n = 5) and SHR (n = 5) arterial myocytes before and after Gö6976. (E) Relative Cav1.2 expression in NT vs. SHR arteries. Relative Cav1.2 mRNA expression was determined by real-time RT-PCR, normalized to β-actin and expressed as fold increase relative to β-actin. \*, P < 0.05.

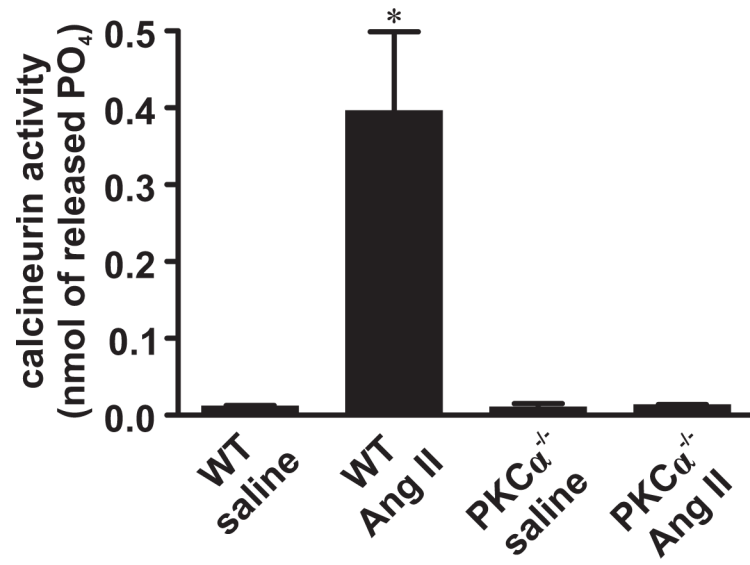


**Fig. S4.** PKC $\alpha$  increases calcineurin activity during AngII-induced hypertension. (A) Bar plot of the mean  $\pm$  SEM of calcineurin activity in arterial myocytes from saline- and AngII-infused WT and PKC $\alpha$ <sup>-/-</sup> mice. \*,  $P < 0.05$ .

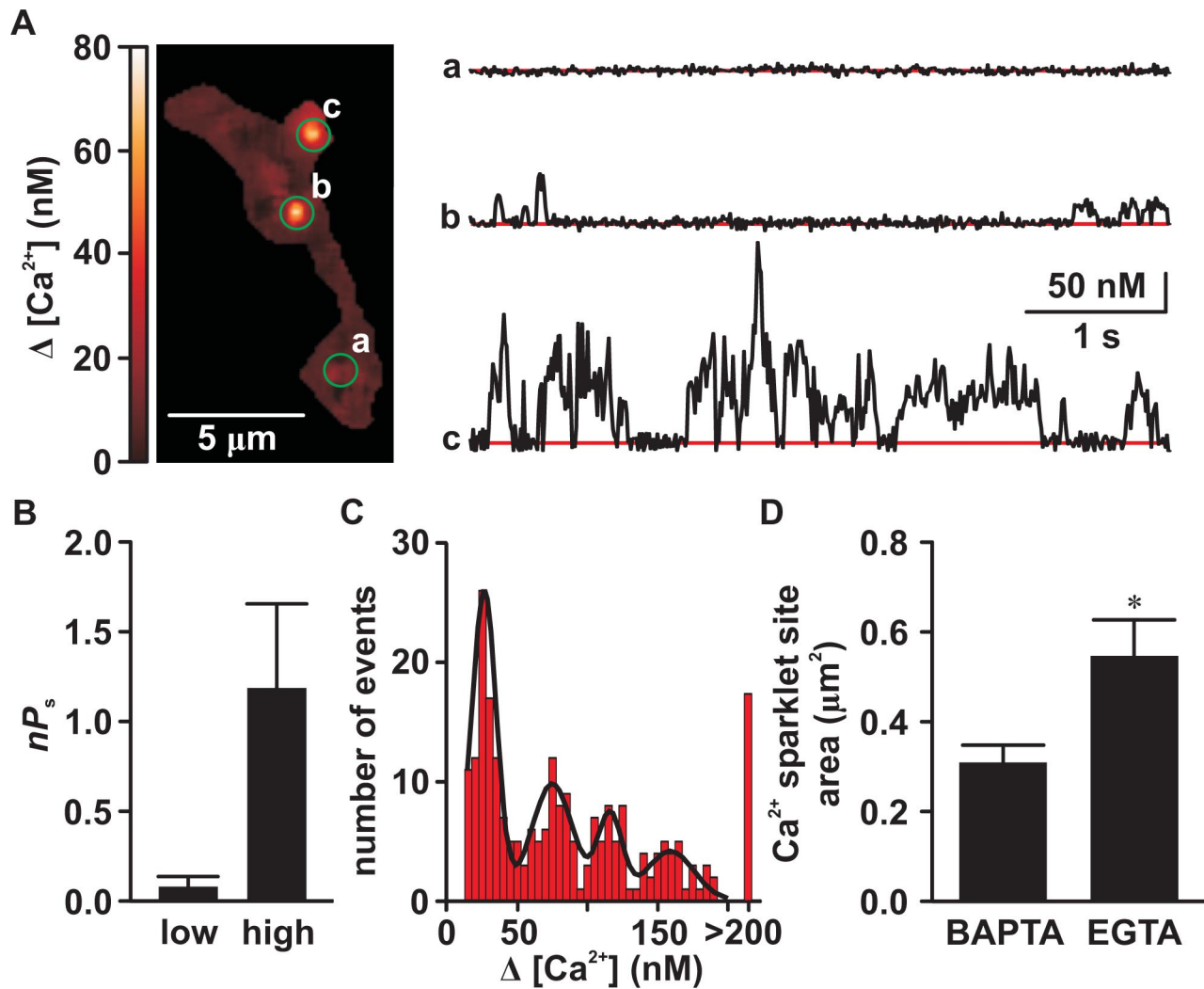


**Fig. S5.**  $Ca^{2+}$  sparklets in arterial myocytes loaded with the fast  $Ca^{2+}$  buffer BAPTA. (A) TIRF image of an arterial myocyte (holding potential =  $-70$  mV) loaded with the fluorescent  $Ca^{2+}$  indicator Fluo-5F (0.25 mM) and BAPTA (10 mM) (Left). (Right) Traces show the time course of  $[Ca^{2+}]_i$  in the sites indicated by the green circles before. (B) Bar plot of the mean  $\pm$  SEM  $nP_s$  of low and high  $nP_s$   $Ca^{2+}$  sparklets in myocytes loaded with BAPTA. (C) Amplitude histogram of  $Ca^{2+}$  sparklets in BAPTA-loaded cells. The black line represents the best fit to the data by using the Gaussian function with a quantal unit of  $Ca^{2+}$  influx of 30 nM. (D) Area of  $Ca^{2+}$  sparklet sites in BAPTA-loaded myocytes. \*,  $P < 0.05$ .